

Comparison of CO₂ Wellbore Flow Models Against CO₂ Injection Field Data: Implications for CO₂-based Geothermal Energy Extraction

Kevin P. HAU*¹, Maren BREHME¹, Alireza RANGRIZ SHOKRI², Reza MALAKOOTI³, Erik NICKEL⁴, Rick J. CHALATURNYK², Martin O. SAAR¹

¹Geothermal Energy & Geofluids Group, Institute of Geophysics, Department of Earth and Planetary Sciences, Sonneggstrasse 5, ETH Zurich, 8092, Zurich, Switzerland,
*Corresponding Author with E-Mail: kevin.hau@eaps.ethz.ch

²Department of Civil and Environmental Engineering, University of Alberta, Edmonton, AB, Canada

³Computer Modelling Group Ltd., Oxford, UK

⁴PTRC Sustainable Energy, Regina, SK, Canada

Keywords:

Wellbore Modelling, CO₂ Injection, Carbon Capture and Storage (CCS), Aquistore CCS Project

ABSTRACT

The accurate prediction of bottomhole conditions in wellbore modelling is critical for the safe and efficient design of subsurface systems involving fluid injection or production. While current wellbore models have been extensively validated using oil and gas operational data, their applicability to pure CO₂, especially under the dynamic conditions present in Carbon Capture and Storage (CCS) projects as well as CO₂-based geothermal energy extraction, remains uncertain.

As CCS deployment accelerates globally, it becomes increasingly important to ensure that these models can accurately represent the rapidly changing thermophysical properties of CO₂ during operation. To address this knowledge gap, this work compares measured field data from the Aquistore CO₂ injection well with software-predicted bottomhole conditions.

1. INTRODUCTION

Global efforts to mitigate the climate crisis are driving a transition towards decarbonised energy systems and economies (IPCC, 2023). While renewable energy sources such as wind, solar, and geothermal will be essential components of this transition, technologies that directly reduce carbon emissions, particularly from hard-to-decarbonise sectors, such as cement, steel, chemicals, and transportation, are equally important (Paltsev et al., 2021).

Among these, Carbon Capture and Storage (CCS) has been proposed as a key technology, enabling the capture of CO₂ at significant point sources and its permanent sequestration in deep geological formations (Global CCS Institute, 2024; IPCC, 2023; Movahedzadeh et al., 2021).

As CCS deployment increases worldwide, accurate modelling of CO₂ behaviour in the subsurface becomes increasingly important (Global CCS Institute, 2024). Although many studies have focused on CO₂ injection and migration within reservoirs (e.g. Kucuk et al., In Review; Hau et al., 2025; Ezekiel et al., 2024; Yalcin et al., 2024; Norouzi et al., 2023; Rangriz Shokri & Chalaturnyk, 2021; Garapati et al., 2015; Randolph & Saar, 2011) relatively few have examined in detail how CO₂ behaves within the (injection) wellbore itself. This is a critical component of subsurface modelling, especially given the unique thermophysical characteristics of CO₂.

Wellbore pressure drop correlations, many of which have been developed and validated using oil and gas production data, have not yet been systematically assessed for CO₂ injection scenarios. CO₂ exhibits a strongly pressure- and temperature-dependent behaviour, characterized by rapid changes in mass density or viscosity (Bachu, 2005). Therefore, wellbore models used for CCS applications must be sensitive enough to capture these variations accurately.

Another challenge is the limited availability of field data from active CO₂ injection wells, which makes it difficult to calibrate or validate existing wellbore models for CO₂-specific conditions. This introduces uncertainty in predicting key performance metrics such as injectivity, thermal effects, and well integrity.

To address this gap, we compare measured CO₂ injection well data with simulated well profiles generated using a simplified single-phase well fluid flow model implemented in industry-standard simulation software CMG-CoFlow. This comparison aims to provide a first estimate on the accuracy and limitations of existing models under CO₂-specific flow conditions and to provide guidance for improving wellbore flow predictions in CCS applications.

2. THE AQUISTORE CCS PROJECT

2.1. Site Description

The Aquestore CCS project, located in southern Saskatchewan, Canada, has been in operation since 2015. Aquestore serves as a commercial-scale research site for the study of CO₂ sequestration in deep hypersaline reservoirs (Movahedzadeh et al., 2021). The project is owned by SaskPower and managed by the Sustainable Energy division of the Petroleum Technology Research Centre (PTRC). CO₂ is sourced from the nearby coal-fired Boundary Dam Power Station and transported to the site for injection via pipeline.

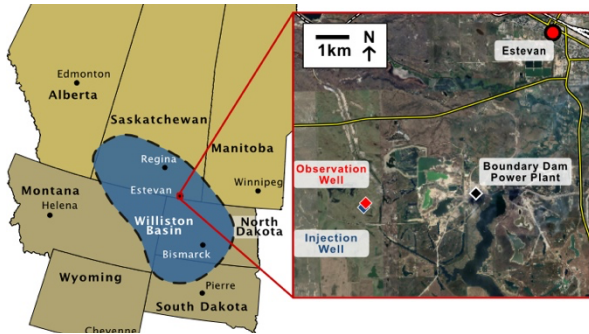


Figure 1: Satellite image of the Aquestore CCS project site, along with a conceptual map illustrating the extent of the North American Williston Basin (after Hau et al., 2025).

A regional overview and a detailed satellite image of the Aquestore site is shown in Figure 1. Two wells exist at the Aquestore CCS site, an injection and an observation well, spaced 151 metres apart. Both are drilled to a depth of approximately 3'400 metres. CO₂ is injected into the hypersaline reservoir of the Deadwood Formation with an average reservoir temperature of around 113°C. The Deadwood Formation lies within the Williston Basin, a major intracratonic basin in Canada (Movahedzadeh et al., 2021).

Both wells are equipped with a broad variety of instruments and sensors. The observation well is equipped with instruments to monitor pressure and temperature changes in response to CO₂ injection. A range of monitoring techniques, including fibre-optic sensors and geophysical surveys, is employed to observe reservoir behaviour and evaluate storage performance (Movahedzadeh et al., 2021). Detailed information on the well completion can be found in Subsection 2.2.

2.2. CO₂ Injection Well Completion

Figure 2 presents a schematic drawing of the Aquestore CO₂ injection well (Global CCS Institute, 2015): The injection well consists of a 10 5/8 in. main borehole drilled to a total depth of 3'396 metres. A 7 5/8 in casing is installed and cemented in place within the hole, using CO₂-resistant cement to ensure long-term well integrity. Inside the casing, a 4 1/2-inch tubing is installed.

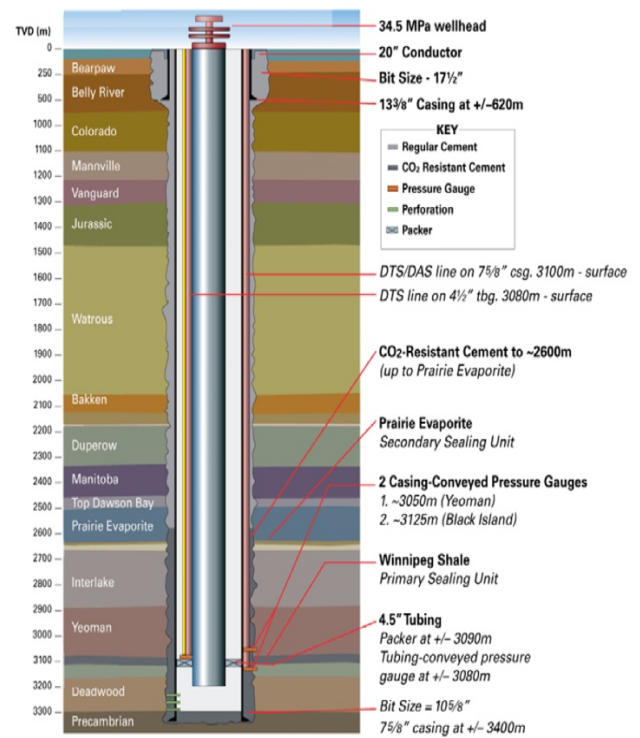


Figure 2: Completion schematic of the Aquestore CO₂ injection well, including casing and tubing configurations, and monitoring methods (Global CCS Institute, 2015).

A packer system is set at a depth of around 3'090 metres, within the Icebox Member, to isolate the injection zone and control the flow of CO₂ into the target formation.

Distributed Temperature Sensing (DTS) and Distributed Acoustic Sensing (DAS) systems are deployed along the full length of the well, mounted on both the casing and the tubing, enabling continuous monitoring of temperature and pressure (Movahedzadeh et al., 2021).

3. METHODS

This study modelled the injection of pure CO₂, predicted bottomhole pressure and temperature conditions in the injection well, and compared the results against four measured field samples of the Aquestore CCS project. A simplified wellbore structure (see Section 3.5) was adopted in place of the detailed existing completion design, visible in Figure 2.

3.1. Aquestore Data Samples

Operational data were provided by PTRC Sustainable Energy, consisting of four data samples collected during active CO₂ injection at the Aquestore project. Each sample consists of the measured CO₂ mass flow rate (*m*), together with the measured wellhead pressure and temperature (WHP, WHT) and bottomhole pressure and temperature (BHP, BHT). The four samples are summarised in Table 2 and enable the comparison of the measured data with the modelled wellbore pressure and temperature profiles.

3.2 Wellbore Simulation Setup

Wellbore simulations were performed using CoFlow, an Integrated Production System Modelling (IPSM) software developed by Computer Modelling Group Ltd. (CMG). The Peng-Robinson Equation of State (Peng & Robinson, 1976) Click or tap here to enter text. was used to accurately calculate the thermophysical properties of CO₂, including its strongly pressure- and temperature-dependent mass density and viscosity.

For each sample, the measured wellhead pressure and temperature were used as boundary conditions to initialise the pressure/temperature profile calculation at the surface. The pressure profile for pure CO₂ along the wellbore was computed using the pressure drop formulation described in Section 3.3, while the temperature distribution was determined following the methodology detailed in Section 3.4. Model predictions of pressure and temperature were subsequently benchmarked against field data, enabling a first assessment of the CoFlow's ability to replicate observed CO₂ injection behaviour.

3.3 Pressure Profile Calculation

Starting with steady-state momentum conservation equation in pipes, the overall pressure change along a wellbore, ΔP , can be decomposed into three pressure change components: the hydrostatic pressure change, the kinematic pressure change, and the frictional pressure change, as shown in Equation (1):

$$\Delta P = \Delta P_{Hydrostatic} + \Delta P_{Kinematic} + \Delta P_{Friction} \quad [1]$$

The hydrostatic component represents the gravitational head of the fluid column and often the most dominant of the pressure change components. The kinematic component accounts for changes in fluid momentum along the flow path, becoming significant when compressibility effects or velocity variations are large. The frictional component captures energy losses due to wall shear, which depend on fluid velocity, viscosity, pipe roughness, and flow regime.

The overall pressure change for pure gas wells along a wellbore can be calculated as follows (Computer Modelling Group Ltd., 2025):

$$\frac{\Delta P}{\Delta L} = \rho g \sin\theta + \rho \left(v \frac{\Delta v}{\Delta L} \right) + \frac{f_D \rho v^2}{2D} \quad [2]$$

Table 1: Assumed material properties for the CO₂ injection well.

Inside Diameter [cm]	Wall Thickness [cm]	Roughness [m]	Thermal Conductivity [W/(m K)]	Material Type
9.7	0.86	4.6×10^{-5}	45	Carbon Steel

Table 2: Measured wellhead (WHP/WHT) and bottomhole pressure and temperature (BHP/BHT) for the four sampled CO₂ injection mass flow rates (\dot{m}) (Rangriz Shokri et al., 2021).

Sample	\dot{m} [kg/sec]	WHP _{measured} [kPa]	WHT _{measured} [°C]	BHP _{measured} [kPa]	BHT _{measured} [°C]
1	5.8	8644.9	11.1	35'734.1	76.2
2	2.9	9167.1	9.9	36'078.5	82.9
3	0.9	9814.5	10	35'733.9	93.5
4	0.1	10992.1	28.3	34'964.9	101.5

With:

$$\begin{aligned} P &= \text{pressure [Pa]} \\ L &= \text{pipe section length [m]}, \\ \rho &= \text{gas mass density [kg/m}^3\text{]} \\ g &= \text{gravitational constant [m/sec}^2\text{]}, \\ \theta &= \text{well inclination angle [}^\circ\text{]} \\ v &= \text{average flowing velocity [m/s]}, \\ f_D &= \text{Darcy friction factor [-]}, \\ D &= \text{pipe diameter [m]} \end{aligned}$$

In general, the thermophysical properties of gases usually vary strongly with both pressure and temperature, therefore Equation (2) cannot be integrated over the entire well length. Instead, any well must be discretised into sufficiently small segments, within which gas properties can be considered constant.

3.4 Temperature Profile Calculation

The temperature change of the injected fluid along the wellbore depends on the ambient geothermal temperature, the inlet fluid temperature, the flow regime within the wellbore, and the heat transfer between the fluid and the surrounding formation. The standard steady-state energy conservation equation in pipes is used to model the heat transfer between the fluid inside the wellbore and the surrounding formation. The energy balance is normally stated as shown in Equation (3) (Hasan & Kabir, 2018):

$$\begin{aligned} &(Q_{convection} + E_{Potential} + E_{Kinetic})_{Pipe-inlet} \\ &\quad + Q_{conduction,formation} \\ &= \\ &(Q_{convection} + E_{Potential} + E_{Kinetic})_{Pipe-outlet} \quad [3] \end{aligned}$$

With:

$$\begin{aligned} Q_{convection} &= \text{convective heat flow,} \\ E_{potential} &= \text{potential energy,} \\ E_{kinetic} &= \text{kinetic energy,} \\ Q_{conduction,formation} &= \text{formation conduction heat} \end{aligned}$$

3.5 Wellbore Geometry and Material Properties

A simplified wellbore design was implemented in the simulations to represent the injection well. The tubing was modelled as a cylindrical conduit with a measured depth of 3233 m. The tubing dimensions and material properties are summarised in Table 1.

4 RESULTS AND DISCUSSION

This section compares the measured Aquistore field data with the predicted wellbore pressure and temperature profiles, computed using the methodology described in Section 3. Since the prediction of the well pressure profiles depends on the choice of pressure change model, it is important to note that several well-established models available within the software have been tested as part of this work. These include the Beggs & Brill (1973) and its modified version by Payne et al. (1979), the Duns & Ros model (1963), Gray’s model (1978), the Hagedorn and Brown’s model (1965), as well as a physics-based model approach such as the model by Kaya et al. (1999)

In the presented study, however, the injection of pure CO₂ results in identical predicted pressure profiles across all these models. For this reason, no single model is highlighted in the following discussion. It should also be noted that the results presented here are based entirely on uncalibrated wellbore models. The intention is to investigate the inherent behaviour of the original pressure and temperature change models, without the influence of any model tuning. The resulting software-predicted bottomhole pressures (BHP) and temperatures (BHT) for each of the four CO₂ injection mass flow rate samples (\dot{m}) are summarised in Table 3. Figures 3 and 4 present the measured and predicted pressure and temperature profiles along the injection well.

Table 3: Predicted bottomhole pressure (BHP) and temperature (BHT) for the four sampled CO₂ injection mass flow rates (\dot{m}).

Sample	\dot{m} [kg/sec]	BHP _{pred} [kPa]	BHT _{pred} [°C]
1	5.8	36’244.4	60.8
2	2.9	36’660.6	73.9
3	0.9	36’612.2	96.7
4	0.1	36’430.4	107.2

Figure 3 shows the measured wellhead and bottomhole pressures (color-coded markers) and the corresponding predicted pressure profiles (color-coded lines), with a zoomed inset highlighting the bottomhole region between 2’500 m and 3’500 m well depth. Figure 4 presents measured and predicted temperatures in a similar format, including the ambient geothermal temperature (solid black line) for reference.

Table 4: Differences between measured and predicted bottomhole pressures (ΔP) and temperatures (ΔT) for all samples.

Sample	\dot{m} [kg/sec]	ΔP [kPa]	ΔP [%]	ΔT [°C]	ΔT [%]
1	5.8	510.3	1.4	15.4	20.2
2	2.9	582.1	1.6	9.0	10.8
3	0.9	878.3	2.5	-3.2	-3.5
4	0.1	1465.5	4.2	-5.7	-5.6

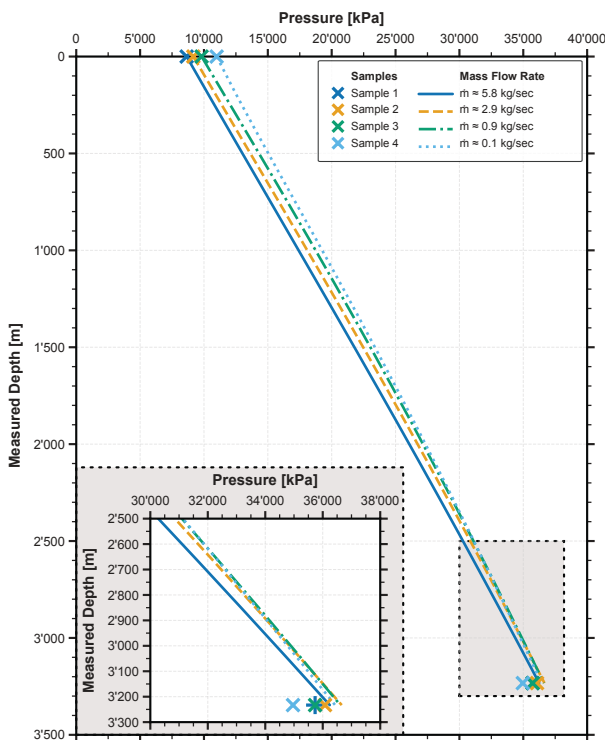


Figure 3: Wellhead and bottomhole pressures for four CO₂ injection flow rates. Measured data are markers; software-predicted profiles are lines. The inset figure highlights the bottomhole region.

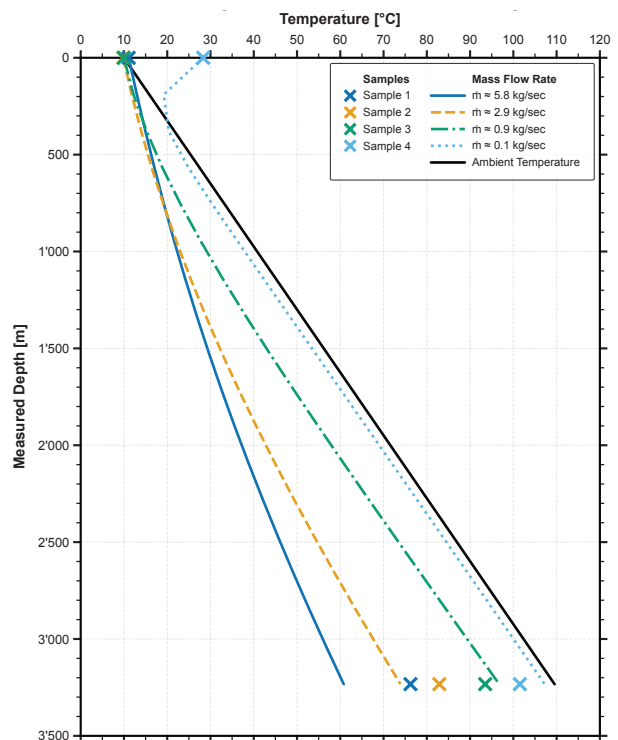


Figure 4: Wellhead and bottomhole temperatures for four CO₂ injection samples. Measured data are markers; software-predicted profiles are lines. The ambient temperature is plotted in black.

Table 4 summarises the differences between measured and predicted bottomhole pressure (ΔP) and temperature values (ΔT) for the four data samples. Positive values in the table indicate an overprediction of the bottomhole value, while negative values represent an underprediction.

4.1 Pressure Profiles

Overall, the bottomhole pressures are generally well predicted, although the pressure drop model consistently overpredicts the BHP. Differences between measured and predicted pressures values range from 1.4% to 4.2%, with larger deviations observed at lower mass flow rates (see Table 4). Figure 5 shows measured and predicted bottomhole pressures for all four mass flow rates. Each pair of values (predicted vs. measured) is connected by a dashed line, with filled markers representing measured data (see Table 2) and open markers indicating predicted values (see Table 3). Note that the x-axis displays mass flow rates in increasing order, so the first point corresponds to Sample 4, which has the lowest mass flow rate, while Sample 1, with the highest mass flow rate, appears last.

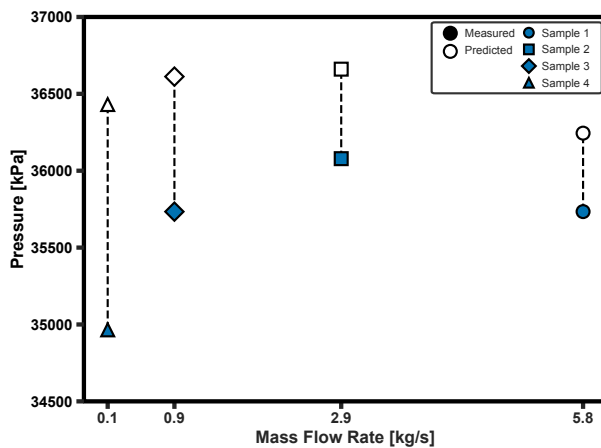


Figure 5: Measured (filled) and predicted (open) bottomhole pressure as a function of mass flow rate. Marker shapes indicate samples; dashed lines connect measured and predicted temperature pairs.

The systematic BHP overprediction can be attributed to several modelling assumptions. First, the simulations assume pure CO_2 , while the actual injection stream may contain minor impurities, such as N_2 , O_2 , H_2O . Impurities alter the well fluid's bulk mass density, viscosity, and compressibility relative to pure CO_2 . Second, a simplified wellbore geometry was used in the model, omitting details such as changes in tubing, packers, or localised restrictions of the flow area, for example from salt precipitation. Any of those features can influence the pressure distribution along the well. Third, thermal processes were modelled using the approach described in Section 3.4. This is relevant because the thermophysical properties of CO_2 are strongly dependent to both pressure and temperature. Thus, even small temperature variations along the wellbore can affect fluid mass density, and hence the hydrostatic pressure gradient, as well as the fluids

viscosity, which controls frictional losses. Consequently, simplifications in the temperature calculation may indirectly contribute to discrepancies in the predicted pressure profile. Finally, small uncertainties are inevitable for the bottomhole pressure and temperature measurements, given the technical challenges of acquiring accurate data at depths exceeding 3 km.

Despite these limitations, a slight overprediction of BHP may be acceptable when no measurements are available, such as when downhole gauges are not operational. A systematic overprediction of the BHP potentially reduces the risk of accidentally fracturing the reservoir or cap rock compromising formation integrity, although it may slightly underestimate the achievable injectivity.

4.2 Temperature Profiles

Unlike the pressure profiles, the temperature predictions do not display a consistent trend of over- or underestimation. Instead, the direction of the difference seems to correlate with the mass flow rate. For higher injection rates (Sample 1 and 2), the software underpredicts the bottomhole temperature, with differences of up to 20.2% (see Table 4). Conversely, at lower flow rates (Samples 3 and 4), the model overpredicts the bottomhole temperature by up to 5.6%. This indicates the need to more accurately include the thermal exchange between the injected CO_2 and the surrounding rock.

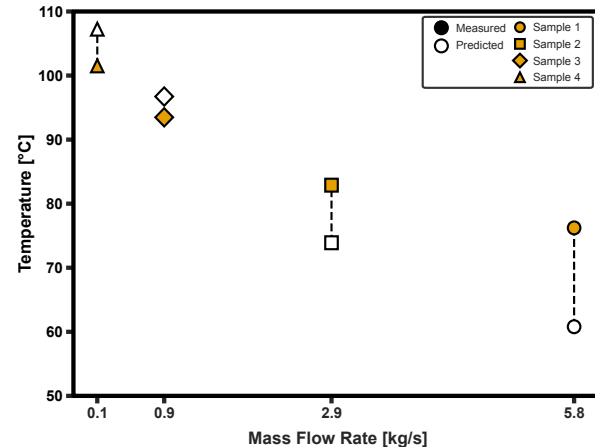


Figure 6: Measured (filled) and predicted (open) bottomhole temperature as a function of mass flow rate. Marker shapes indicate samples; dashed lines connect measured and predicted temperature pairs.

Figure 6 shows these observations as pairs of temperature values (predicted vs. measured). Identical to Figure 5, each data pair is connected by a dashed line, with filled markers representing measured data (see Table 2) and open markers indicating predicted values (see Table 3). As in Figure 5, the x-axis displays mass flow rates in increasing order, such that the first point corresponds to Sample 4 with the lowest mass flow rate, while Sample 1, with the highest mass flow rate, appears last.

The mismatch between predicted and measured bottomhole temperatures highlights the limitations of the simplified, uncalibrated thermal modelling assumptions applied in this initial test. Since CO₂ thermophysical properties are highly sensitive to temperature, these simplifications may also contribute indirectly to the discrepancies observed in the pressure predictions discussed in Section 4.1.

Overall, while the general trends of the temperature profiles are reproduced, the magnitude of the deviations indicates that calibration of the thermal model is required.

5. CONCLUSION

This study compared measured Aquistore field data with simulated wellbore pressure and temperature profiles during single-phase CO₂ injection. The used single-phase CO₂ model overpredicted bottomhole pressures for all four data samples. Temperature predictions, however, showed inconsistent agreement, with underestimation at high injection rates and overestimation at low rates, reflecting limitations of the simplified, uncalibrated thermal model. These discrepancies underscore the need for more robust wellbore flow models when applied to CO₂ injection scenarios. Such improvements are critical for reliably assessing the feasibility and performance of CO₂-based geothermal energy extraction. Future work will focus on refining the thermal representation, evaluating industry-standard two-phase flow correlations in CoFlow, and applying the methodology to larger datasets from different sites and well configurations, including both CO₂ storage and CO₂-EOR operations.

DECLARATION OF AI USAGE

The authors declare the usage of OpenAI's ChatGPT (GPT-5) to assist in editing, refining, and improving the clarity of the manuscript text. The scientific content, data analysis, results, and conclusions were generated entirely by the authors.

ACKNOWLEDGEMENTS

We gratefully acknowledge the support of the Werner Siemens Foundation (Werner Siemens-Stiftung) for its funding of the Geothermal Energy and Geofluids (GEG.ethz.ch) group at ETH Zurich, Switzerland. Additionally, we thank the Energi Simulation Foundation for their support. We also extend our gratitude to Computer Modelling Group Ltd. for supplying the CoFlow software package.

BIBLIOGRAPHY

- Beggs, D. H., & Brill, J. P. (1973). A Study of Two-Phase Flow in Inclined Pipes. *Journal of Petroleum Technology*, 25(05), 607–617. <https://doi.org/10.2118/4007-PA>
- Computer Modelling Group Ltd. (2025). *CoFlow Version 2025.30* (2025.30). Computer Modelling Group Ltd.
- Duns, H., & Ros, N. C. J. (1963). Vertical flow of gas and liquid mixtures in wells. *6th World Petroleum Congress*, WPC-10132. <http://onepetro.org/WPCONGRESS/proceedings-pdf/WPC06/All-WPC06/WPC-10132/2079811/wpc-10132.pdf/1>
- Ezekiel, J., Vahrenkamp, V., Hoteit, H. A., Finkbeiner, T., & Mai, P. M. (2024). Techno-economic assessment of large-scale sedimentary basin stored-CO₂ geothermal power generation. *Applied Energy*, 376. <https://doi.org/10.1016/j.apenergy.2024.124270>
- Garapati, N., Randolph, J. B., & Saar, M. O. (2015). Brine displacement by CO₂, energy extraction rates, and lifespan of a CO₂-limited CO₂-Plume Geothermal (CPG) system with a horizontal production well. *Geothermics*, 55, 182–194. <https://doi.org/10.1016/j.geothermics.2015.02.005>
- Global CCS Institute. (2015). *Aquistore - CO₂ Storage at the World's First Integrated CCS Project*. <http://www.ptre.ca>
- Global CCS Institute. (2024). *Global status of CCS 2024*.
- Gray, H. E. (1978). Vertical Flow Correlation in Gas Wells. In *User's Manual for API 14B Surface Controlled Subsurface Safety Valve Sizing Computer Program*. American Petroleum Institute.
- Hagedorn, A. R., & Brown, K. E. (1965). Experimental Study of Pressure Gradients Occurring During Continuous Two-Phase Flow in Small-Diameter Vertical Conduits. *Journal of Petroleum Technology*, 17(04), 475–484. <https://doi.org/10.2118/940-PA>
- Hasan, R., & Kabir, S. (2018). *Fluid Flow and Heat Transfers in Wellbores*. Society of Petroleum Engineers (SPE). <https://doi.org/10.2118/9781613995457>
- Hau, K. P., Brehme, M., Rangriz Shokri, A., Malakooti, R., Nickel, E., Chalaturnyk, R. J., & Saar, M. O. (2025a). CCS coupled with CO₂ plume geothermal operations: Enhancing CO₂ sequestration and reducing risks. *Geothermics*, 133, 103447. <https://doi.org/10.1016/j.geothermics.2025.103447>
- Hau, K. P., Brehme, M., Rangriz Shokri, A., Malakooti, R., Nickel, E., Chalaturnyk, R., & Saar, M. O. (2025b). CCS Coupled with CO₂ Plume Geothermal Operations: Enhancing CO₂ Sequestration and Reducing Risks. *Geothermics (In Review)*.
- IPCC. (2023). *Climate Change 2023: Synthesis Report. Contribution of Working Groups I, II and III to the Sixth Assessment Report of the Intergovernmental Panel on Climate Change [Core Writing Team, H. Lee and J. Romero (eds.)]*. IPCC, Geneva, Switzerland. (P. Arias, M. Bustamante, I. Elgizouli, G. Flato, M. Howden, C. Méndez-Vallejo, J. J. Pereira, R. Pichs-Madruga, S. K. Rose, Y. Saheb, R. Sánchez Rodríguez,

- D. Üрге-Vorsatz, C. Xiao, N. Yassaa, J. Romero, J. Kim, E. F. Haites, Y. Jung, R. Stavins, ... C. Péan, Eds.). <https://doi.org/10.59327/IPCC/AR6-9789291691647>
- Kaya, A. S., Sarica, C., & Brill, J. P. (1999, October 3). Comprehensive Mechanistic Modeling of Two-Phase Flow in Deviated Wells. *SPE Annual Technical Conference and Exhibition*. <https://doi.org/10.2118/56522-MS>
- Kucuk, S., Farajzadeh, R., Brehme, M., Rossen, W. R., & Saar, M. O. (n.d.). CO₂-Plume Geothermal (CPG) After Enhanced Oil Recovery (EOR). *Applied Energy (in Review)*.
- Movahedzadeh, Z., Shokri, A. R., Chalaturnyk, R., Nickel, E., & Sacuta, N. (2021). Measurement, monitoring, verification and modelling at the Aquistore CO₂ storage site. *First Break*, 39(2), 69–75. <https://doi.org/10.3997/1365-2397.fb2021013>
- Norouzi, A. M., Pouranian, F., Rabbani, A., Fowler, N., Gluyas, J., Niasar, V., Ezekiel, J., & Babaei, M. (2023). CO₂-plume geothermal: Power net generation from 3D fluvial aquifers. *Applied Energy*, 332. <https://doi.org/10.1016/j.apenergy.2022.120546>
- Paltsev, S., Morris, J., Kheshgi, H., & Herzog, H. (2021). Hard-to-Abate Sectors: The role of industrial carbon capture and storage (CCS) in emission mitigation. *Applied Energy*, 300. <https://doi.org/10.1016/j.apenergy.2021.117322>
- Payne, G. A., Palmer, C. M., Brill, J. P., & Beggs, H. D. (1979). Evaluation of Inclined-Pipe, Two-Phase Liquid Holdup and Pressure-Loss Correlation Using Experimental Data (includes associated paper 8782). *Journal of Petroleum Technology*, 31(09), 1198–1208. <https://doi.org/10.2118/6874-PA>
- Peng, D.-Y., & Robinson, D. B. (1976). A New Two-Constant Equation of State. *Industrial & Engineering Chemistry Fundamentals*, 15(1), 59–64. <https://doi.org/10.1021/i160057a011>
- Randolph, J. B., & Saar, M. O. (2011). Combining geothermal energy capture with geologic carbon dioxide sequestration. *Geophysical Research Letters*, 38(10). <https://doi.org/10.1029/2011GL047265>
- Rangriz Shokri, A., & Chalaturnyk, R. (2021). *Feasibility Study for Proposed CO₂ Circulation Test at the Aquistore Injection Site, Saskatchewan*. www.bfe.admin.ch
- Rangriz Shokri, A., Talman, S., Chalaturnyk, R. J., & Nickel, E. (2021, June). On the Temporal Evolution of Non-Isothermal Injectivity Behaviour at an Active CO₂ Injection Site. *55th U.S. Rock Mechanics/Geomechanics Symposium*. <https://onepetro.org/ARMAUSRMS/proceedings/ARMA21/All-ARMA21/ARMA-2021-1762/468120>
- Span, R., & Wagner, W. (1996). A new equation of state for carbon dioxide covering the fluid region from the triple-point temperature to 1100 K at pressures up to 800 MPa. *Journal of Physical and Chemical Reference Data*, 25(6), 1509–1596. <https://doi.org/10.1063/1.555991>
- Yalcin, B., Ezekiel, J., & Mai, P. M. (2024). Potential for CO₂ plume geothermal and CO₂ storage in an onshore Red Sea Rift basin, Al-Wajj, Saudi Arabia: 3D reservoir modeling and simulations. *Geothermics*, 119. <https://doi.org/10.1016/j.geothermics.2024.102966>